

POWER DEPENDENCE OF POLYCRYSTALLINE SILICON THIN FILM CRYSTALLINITIES WITH MULTILINE BEAM CONTINUOUS-WAVE LASER LATERAL CRYSTALLIZATION

Nguyen Thi Thuy¹, Nguyen Thi Huyen¹, Pham Thi Dung¹, Tran Manh Cuong¹,
Trinh Duc Thien¹ and Shin-Ichiro Kuroki²

¹*Faculty of Physics, Hanoi National University of Education*

²*Research Institute for Nanodevice and Bio System, Hiroshima University*

Abstract. Polycrystalline Silicon Thin Film Transistors (poly-Si TFTs) have been played as important driving elements for Flat panel display (FPD). In this work, we studied crystallinities of laser-crystallized poly-Si thin films using Multi-Line Beam (MLB) –CLC and investigated the dependence of poly-Si thin films on the conditions of laser power along with scanning speed. Surface orientation of poly-Si thin films were observed by X-Ray Diffraction (XRD) and Electron Back Scattering Diffraction (EBSD) measurement. In addition, the stress values of poly-Si thin films varied with laser powers were calculated from Raman spectra. We found that highly (100)-surface oriented poly-Si thin films were obtained as changing the laser power along with changing scanning speeds from 5 W to 7 W. The poly-Si thin films formed at low laser power values had better (100)-surface orientation.

Keywords: Poly-Si thin film, CLC, TFTs, LTPS-TFTs, Laser Crystallization

1. Introduction

Flat panel display (FPD) technologies such as Liquid Crystal Display (LCD), Active Matrix Organic Light Emitting Diode (AMOLED), and Quantum Light Emitting Diode (QLED) displays have been rapidly developed for recent decades. Display's resolution plays an important role in the FPD market and has a high competition between manufactures. Moreover, three-dimensional (3D) electronics and glass sheet computers are the key objective of computer manufactures in the world. Thin film transistors (TFTs) fabricated on glass and transparent flexible substrates play as the basic driving elements of the FPDs [1]. Improving the performance and electrical properties of TFTs and reducing their cost for practical applications have been attracted much attention.

Received October 15, 2019. Revised October 22, 2019. Accepted October 29, 2019.

Contact Nguyen Thi Thuy, e-mail address: nguyenthuy@hnue.edu.vn

Low-temperature polycrystalline silicon (LTPS)-TFTs have been widely applied in the largest manufacturing companies in the world such as Apple, Sony, Samsung, etc. due to their high performance, excellent reliability, and low cost [2-3]. Crystallinities of polycrystalline silicon (poly-Si) thin films play an important role for characteristics of the TFTs. Many crystallization technologies including laser annealing and thermal annealing have been applied to form poly-Si thin films. Excimer Laser Annealing (ELA) has been successfully applied to high performance active-matrix TFTs in LCD technology due to its high performance and uniformity of devices. However, their electron mobility is limited below $200 \text{ cm}^2/\text{Vs}$ [2-3]. For ICs applications, the electron mobility needs to be improved to $600 \text{ cm}^2/\text{Vs}$ that is comparable to the mobility of bulk Si devices. Recently, new crystallization technologies such as Sequential Lateral Solidification (SLS), Solid-Phase Crystallization (SPC), Thermal Plasma Jets (TPJ), and Continuous-Wave Laser Lateral Crystallization (CLC) have been developed to improve characteristics of poly-Si thin films and performance of TFTs [4-11]. In this work, we applied a CLC technology with a multiline laser beam to form poly-Si thin films and studied their crystallinities.

2. Content

2.1. Experiments

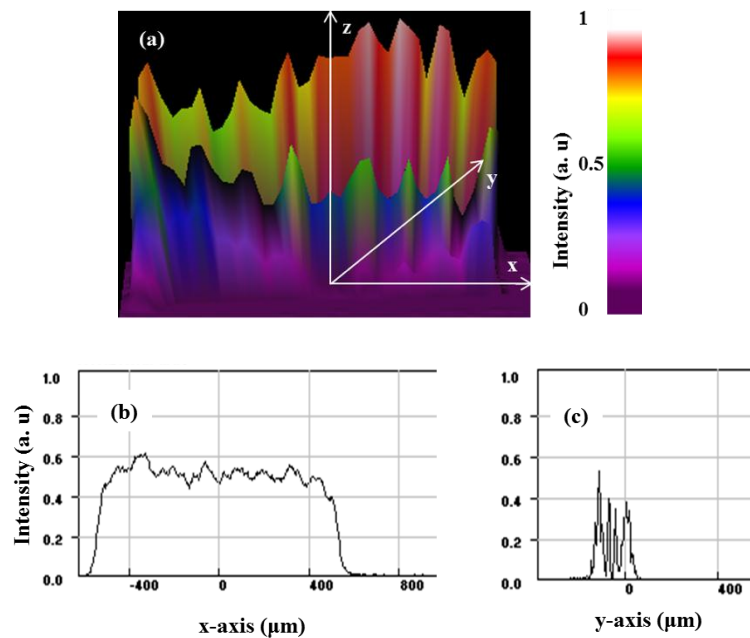


Figure 1. (a) Three-dimensional, (b) Y-cross-sectional, and (c) X-cross-sectional profiles of multiline laser beam

In our study, amorphous Si (a-Si) samples were prepared before being crystallized as follows: An a-Si film of 150 nm thickness deposited at a temperature of 430°C by Plasma-Enhanced Chemical Vapor Deposition (PECVD) on a $1 \mu\text{m}$ thick SiO_2 buffer of

a quartz substrate. The thickness of a-Si was determined by penetration length of laser source with wavelength of 532 nm. Then, a cap SiO₂ of 100 nm thickness were deposited by the PECVD to reduce surface roughness of the film [12]. To reduce the large amount of hydrogen, the film was partially dehydrogenated by furnace annealing at 490°C in N₂ ambient for an hour. Sequentially, laser crystallization process was carried out to form poly-Si thin films with Multi-Line Beam (MLB)-CLC. By absorbing the continuous-wave laser, the a-Si thin films melted and then crystallized as poly-Si thin films. Figure 1(a) shows three dimensional (3D) profile of multiline laser beam with its color chart on the right side of figure. The average intensity of the beam along x-axis was slightly fluctuated and seemed to be locally Gaussian distribution as shown in Fig. 1(b). The fluctuation of laser intensity along x-axis is significantly affected on the uniformity of poly-Si thin films because laser beam is scanned over the films along y-axis. The laser beam is formed into a four-line beam. Every single line beam had Gaussian distribution in intensity.

The laser beam was scanned over the samples with single scans and overlapped scans along y-axis as shown in Fig. 1(a). Before a-Si thin films were irradiated, SiO₂ cap had been etched by a buffered hydrofluoric acid (BHF). Rigaku X-ray diffraction (XRD), Horiba Raman spectroscopy, and electron back scattering diffraction (EBSD) were applied to measure crystallinities of poly-Si thin films.

2.2. Morphology of poly-Si thin films

Figure 2(a) and 2(b) show the microphotographs of poly-Si films crystallized with a single scan and overlapped scan, respectively. A laser power of 5 W and scanning speed of 0.35 cm/s were fixed. A poly-Si and a-Si areas were observed at the left and right sides of the irradiated region shown in Fig. 2(a). Green, yellow, and red color lines appeared in the poly-Si due to the variation of laser intensity along x-axis shown in Fig. 1(a). With overlapped scans, the a-Si area transformed to poly-Si in the full width of irradiated region as shown in Fig. 2(b).

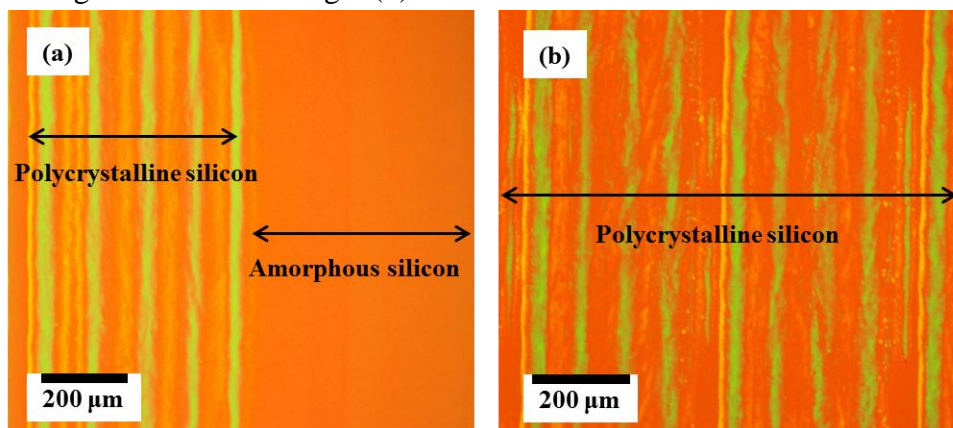


Figure 2. Microphotographs of poly-Si thin films formed by MLB-CLC with (a) a single scan, (b) overlapped scans

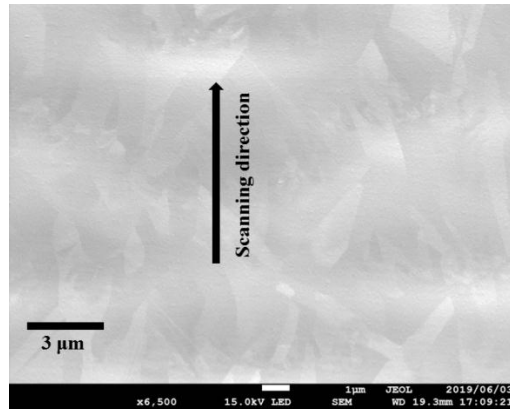


Figure 3. Surface image of a poly-Si thin film formed by MLB-CLC measured by Scanning Electron Microscope (SEM)

Surface morphology of poly-Si thin films were observed by SEM in micrometer size region as shown in Fig. 3. The surface of the film was relatively flat and had no defects. Silicon crystallites were observed with various shapes and sizes. They were continuously developed along the scanning direction. Their average width was approximately 1 to 2 μm and their length was larger 10 μm.

2.3. Surface orientation of poly-Si thin films

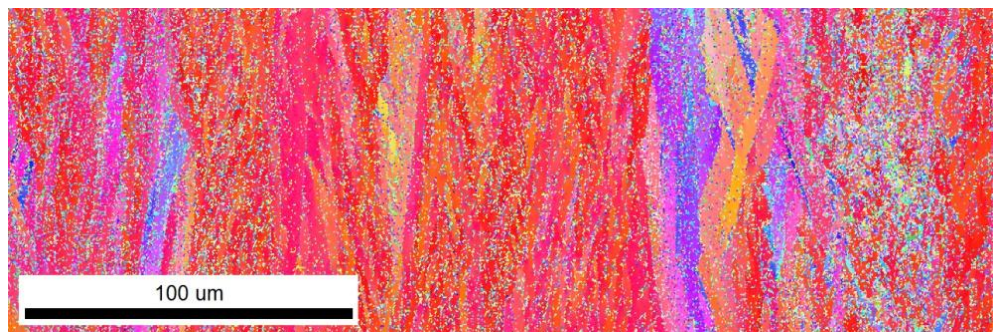


Figure 4. Surface-orientation of a poly-Si thin film formed by MLB-CLC with overlapped scans measured by Electron Back Scattering Diffraction (EBSD)

We observed the surface crystal orientation of poly-Si thin films by EBSD and XRD. The orientation of crystal structures is described by color map in the EBSD result where the red color represents the (100) orientation. Figure 4 shows the orientation mapping of a poly-Si thin film observed in the normal surface direction. For this measurement, crystallization conditions were fixed at 5 W laser power and 0.35 cm/s scanning speed. A polycrystalline silicon region of 100 μm x 300 μm size was randomly measured. It is found that (100) orientation was dominant in the poly-Si thin film.

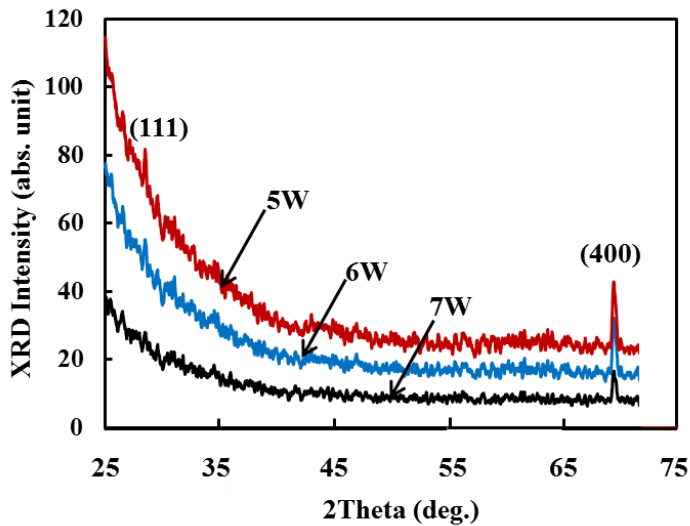


Figure 5. XRD spectra of MLB-CLC poly-Si thin films with various conditions of laser power (5 W, 6 W, 7 W)

In order to form large poly-Si thin films for XRD measurement, we performed overlapping scanning of laser beams with an overlapped region of 400 μm width between two sequential scans along the scanning direction. Figure 5 shows out-of-plane XRD spectra of MLB-CLC poly-Si thin films with three crystallization conditions of laser power along with scanning speed of 5 W, 0.35 cm/s; 6 W; 0.9 cm/s, and 7 W, 1.7 cm/s. Large (400) peaks and small (111) peaks appeared in all three conditions. This result indicates that these poly-Si thin films dominantly exhibited (100) orientation in the normal surface direction over large areas. The XRD intensity of (400) peaks increased as the laser power decreased. It indicates that the preference of (100) surface orientation in poly-Si thin films was better at low laser power range. In our previous report, we formed poly-Si thin films at a fixed laser power of 6 W as changing scanning speed from 0.2 cm/s to 1 cm/s and found that the poly-Si films had dominantly (100)-surface orientation at 0.8 cm/s and 0.9 cm/s scanning speed [11]. In order to form (100)-surface oriented poly-Si thin films at other laser power values, the scanning speed was varied.

2.4. Strain of poly-Si thin films

By absorbing green laser, the a-Si thin film rapidly increased in temperature and melted at its melting point, then the melted silicon was solidified with a drop of temperature. The strain of poly-Si films is induced by the difference between the thermal expansion coefficient of silicon and SiO_2 layers, during heating and cooling processes. The average stress value of poly-Si films can be calculated from their Raman spectra as the equation (1) [13,14].

$$\sigma(\text{GPa}) = -0.25 (\text{GPa}/\text{cm}^{-1}) \times \Delta\omega (\text{cm}^{-1}) \quad (1)$$

Where σ is average stress and $\Delta\omega$ is the shift of Raman peak comparing to unstrained silicon crystals.

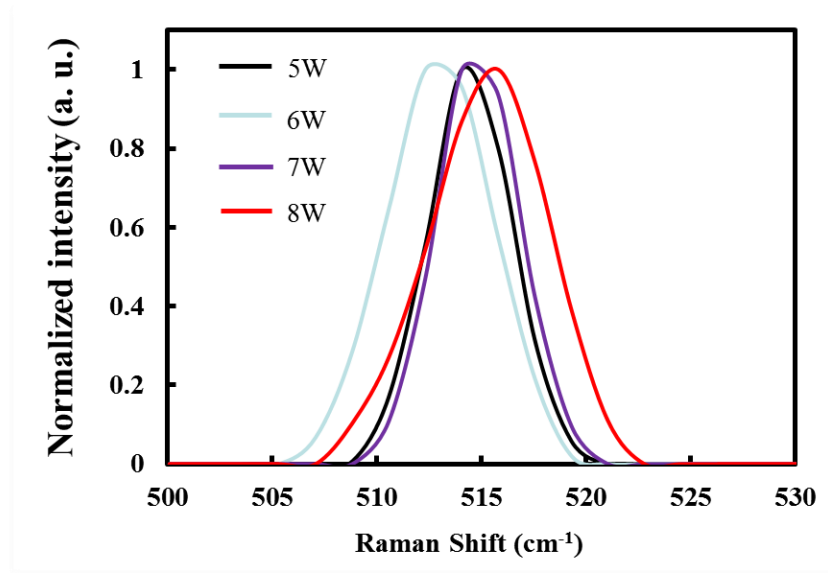


Figure 6. Raman spectra of the MLB-CLC poly-Si thin films with various conditions of laser power (5 W, 6 W, 7 W, 8 W)

Figure 6 shows the micro-Raman spectra of poly-Si thin films. The Raman peaks of poly-Si films were slightly varied and shifted lower than that of single crystal Si (c-Si) at 520 cm^{-1} . Averaged thermal stress values of poly-Si thin films were summarized in the table I. These values were varied from 1.01 GPa to 1.88 GPa. The largest thermal stress value of 1.88 GPa was achieved at 6 W laser power.

Table I. Raman peak shift and stress values of poly-Si thin films versus laser powers

Laser power P(W)	$\Delta\omega$	Tress σ (GPa)
5	-5.779	1.44
6	-7.525	1.88
7	-5.779	1.44
8	-4.033	1.01

The thermal stress in the poly-Si thin films induced tensile strain in the planar direction and compressive strain the depth direction. The relationship between the crystallinity and stress and the effect of thermal strain of poly-Si thin film were discussed in our previous reports [11].

3. Conclusions

In this report, we formed poly-Si thin films using MLB-CLC technology at various conditions of laser power and investigated their crystallinities. The laser power was varied from 5 W to 8 W along with scanning speed to form poly-Si thin films. We carried out XRD and EBSD measurements to observe surface orientation of poly-Si thin films and measuring Raman spectra to calculate their stress values. We found that (400) peaks appeared in all conditions and the largest (400) peak was observed with the

conditions of 5 W laser power and 0.35 cm/s scanning speed. These results indicate that the poly-Si thin films formed at low laser power range had better (100)-surface orientation. In addition, the poly-Si thin films had high thermal stress values of over 1 GPa for all conditions and a maximal value of 1.88 GPa at 6 W laser power.

Acknowledgements: This research was funded by the Ministry of Education and Training, Vietnam (Grant No. B2018-SPH-05-CTrVL). The authors would like to thank Professor S. Higashi and Assistant Professor H. Hanafusa of Hiroshima University for their kind support in the SEM and EBSD measurements. The authors would like to thank Dr. Pham Van Hai of Hanoi National University of Education, Vietnam for his kind support in Raman spectrum measurements.

REFERENCES

- [1] Y. Kuo, 2013. *Electrochem. Soc. Interface*, **55**.
- [2] G. Fotunato, L. Mariucci, R. Carluccio, A. Pecora, V. Forglietti, 2000. *Appl. Surf. Sci.* **154**, 95.
- [3] S. D. Brotherton, D. J. McCulloch, and J. P. Gowers, 2004. *Jpn. J. Appl. Phys.* **43**, 5114.
- [4] C-H Chou, W-S Chan, I-C Lee, C-L. Wang, C-Y Wu, P-Y. Yang, C-Y. Liao, K-Y. Wang, and H-C Cheng, 2015. *IEEE Electron Device Lett.*, **36**, 348.
- [5] J. S. Im, M. Chahal, P.C. van der Wilt, U.J. Chung, G.S. Ganot, A.M. Chitu, N. Kobayashi, K. Ohmori, A.B. Limanov, 2010. *J. Cryst. Growth*, **312**, 2775.
- [6] A. Hara, M. Takei, F. Takeuchi, K. Suga, K. Yoshino, M. Chida, T. Kakehi, Y. Ebiko, Y. Sano, and N. Sasaki, 2004. *Jpn. J. Appl. Phys.* **43**, 1269.
- [7] W-K. Lee, S-M. Han, J. Choi, M-K. Han, 2008. *J. Non-Cryst. Solids*, **354**, 2509.
- [8] S. Morisaki, S. Hayashi, Y. Fujita, S. Higashi, 2014. *J. Display Tech.* **10**, 950.
- [9] M. Yamano, S. Kuroki, T. Sato, and K. Kotani, Jpn., 2014. *J. Appl. Phys.* **53**, 03CC02.
- [10] T. T. Nguyen, M. Hiraiwa, and S.-I. Kuroki, 2017. *Appl. Phys. Express*, **10**(5), 056501.
- [11] T. T. Nguyen, M. Hiraiwa, T. Koganezawa, S. Yasuno, and S.-I. Kuroki, 2018. *Jpn. J. Appl. Phys.* **57**, 031302.
- [12] S. Fujii, S. Kuroki, X. Zhu, M. Numata, K. Kotani, and T. Ito, 2009. *Jpn. J. Appl. Phys.* **48**, 04C129.
- [13] H. Tada, A. Kumpel, R. E. Lathrop, J. B. Slanina, P. Nieva, P. Zavracky, I. N. Miaoulis, and P. Y. Wong, 2000. *J. Appl. Phys.* **87**, 4189.
- [14] H. Kahn, R. Ballarini, A. H. Heuer, 2002. *J. Mater. Res.* **17**, 1855.